Inkjet Printing and Alternative Sintering of Narrow Conductive Tracks on Flexible Substrates for Plastic Electronic Applications

Jolke Perelaer and Ulrich S. Schubert
Friedrich-Schiller-University Jena
Germany

1. Introduction

Although inkjet printers are widely used for graphical applications, it was only within the last decades that inkjet printing has grown to a mature patterning technique. As a consequence, it has gained specific attention in scientific research because of its high precision and its additive nature: only the necessary amount of functional material is dispensed (Tekin *et al.*, 2008). Furthermore, the absence of physical contact between print head and substrate allows many potential applications, such as inkjet printing of labels onto rough curved surfaces, or surfaces that are sensitive to pressure. Inkjet printing is utilised to dose many different kinds of materials, such as conductive polymers and nanoparticles (Osch *et al.*, 2008; Perelaer *et al.*, 2008ab), sol-gel materials (Berg *et al.*, 2007), cells (Derby, 2008), structural polymers (Gans & Schubert, 2004), ceramics (Reis *et al.*, 2005) and even molten metals (Attinger *et al.*, 2000).

Inkjet printing, and in particular drop-on-demand inkjet printing, can compete with lithography techniques, since it places material on demand and in a direct way, which reduces the number of processing steps and the amount of material required, thereby also reducing time, space and waste consumption within production. Furthermore, inkjet printing can also be combined with roll-to-roll production (Forrest, 2004). Typical applications can be seen in the field of plastic electronic devices, which are microelectronic devices that are prepared on flexible polymer substrates, including radio frequency identification tags or electrodes for thin-film transistor circuits.

Similarly, over the few last years, there has been a growing interest in the inkjet printing of conductive materials. One of the compound types that has been frequently used is the poly(3,4-ethylenedioxythiophene):poly(4-styrenesulfonate) (PEDOT:PSS), due to its relatively low costs. However, this polymer does not have a high conductivity (Yoshioka & Jabbour, 2006). Besides conductive polymers, inks that contain metals have been used to create microstructures on polymer substrates (Smith *et al.*, 2006; Kim *et al.*, 2007). It has been shown that inkjet printing of conductive materials is a relatively cheap alternative for the fabrication of electronic devices when compared to other micro- and nanopatterning techniques (Menard *et al.*, 2007), such as photo-lithography (Liu *et al.*, 2005) or laser patterning (Cuk *et al.*, 2000).

Although metals like copper (Hong & Wagner, 2000) and gold (Molesa *et al.*, 2003) have been used for inkjet printing applications, direct inkjet printing of conductive silver tracks onto flexible substrates has gained interest due to silver having the lowest resistivity value and the relatively simple synthesis of silver nanoparticles (Schmid, 2004). Therefore, it has been used for many applications, such as interconnections for a circuitry on a printed circuit board (Szczech *et al.*, 2002), disposable displays and radio frequency identification (RFID) tags (Huang *et al.*, 2004; Potyrailo *et al.*, 2009), organic thin-film transistors (Kim *et al.*, 2007; Gamerith *et al.*, 2007), and electrochromic devices (Shim *et al.*, 2008).

This chapter will describe how inkjet printing techniques can be used for the fabrication of conductive tracks on a polymer substrate. The selective sintering of inkjet printed silver nanoparticles is described by using microwave radiation. This not only sinters the particles into a conductive feature, but it also reduces the sintering time significantly from hours to minutes or even seconds. Furthermore, techniques to improve the printing resolution will be discussed and the fabrication of conductive tracks of 40 µm wide will described.

Before going in detail on inkjet printing of advanced nanoparticle inks, we first review the history of inkjet printing.

2. Historical overview of inkjet printing

The origin of inkjet printing goes back to the eighteenth century when Jean-Antoine Nollet published his experiments on the effect of static electricity on a stream of droplets in 1749 (Nollet & Watson, 1749). Almost a century later, in 1833, Felix Savart discovered the basics for the technique used in modern inkjet printers: an acoustic energy can break up a laminar flow-jet into a train of droplets (Savart, 1833). It was, however, only in 1858 that the first practical inkjet device was invented by William Thomson, later known as Lord Kelvin (Thomson, 1867). This machine was called the *Siphon recorder* and was used for automatic recordings of telegraph messages.

The Belgian physicist Joseph Plateau and the English physicist Lord Rayleigh studied the break-up of liquid streams and are, therefore, seen as the founders of modern inkjet printing technology. The break-up of a liquid jet takes place because the surface energy of a liquid sphere is smaller than that of a cylinder, while having the same volume – see Figure 1 (Goedde & Yuen, 1970).
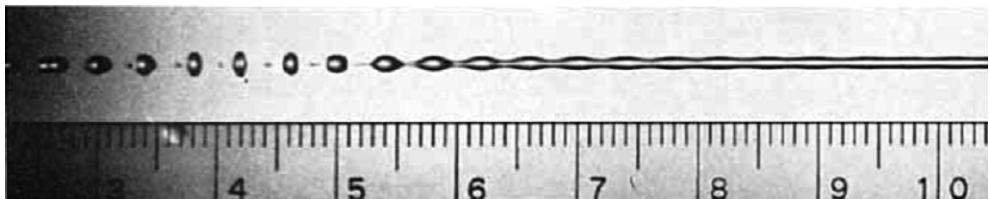

Fig. 1. Break-up of a laminar flow-jet into a train of droplets, because of Rayleigh-Plateau instability (cm scale). Reprinted from (Goedde & Yuen, 1970).

When applying an acoustic energy, the frequency of the mechanical vibrations is approximately equal to the spontaneous drop-formation rate. Subsequently, the drop-formation process is synchronised by the forced mechanical vibration and therefore produces ink drops of uniform mass. Lord Rayleigh calculated a characteristic wavelength λ for a fluid stream and jet orifice diameter d given by (Rayleigh, 1878):

Inkjet Printing and Alternative Sintering of Narrow Conductive Tracks
on Flexible Substrates for Plastic Electronic Applications

267

$$\lambda = 4.443d \qquad (1)$$

The numerical value was later slightly corrected to 4.508 (Bogy, 1979). However, it took another 50 years before the first design of a continuous inkjet printer, based on Rayleigh's findings, was filed as a patent by Rune Elmqvist (Elmqvist, 1951). He developed the first inkjet electrocardiogram printer that was marketed under the name *Mingograf* by Elema-Schönander in Sweden and *Oscillomink* by Siemens in Germany (Kamphoefner, 1972).

In the beginning of the 1960s, two continuous inkjet (CIJ) systems were developed simultaneously, with a difference only in function of the electrical driving signals (Keeling, 1981). The first system was developed by Richard Sweet at Stanford University. He made a high frequency oscillograph, where droplets were formed at a rate of 100 kHz and controlled with respect to their direction by the electrical signal (Sweet, 1965). Later, in 1968, the A. B. Dick Company elaborated upon Sweet's invention to produce a device that was used for character printing and named it the *Videojet 9600*: this was the first commercial continuous inkjet printer. In parallel at the Lund Institute of Technology in Sweden, Hertz *et al.* had developed a similar system where an electrical signal was used to disperse the droplets into a mist, which enables frequencies up to 500 kHz (Hertz & Simonsson, 1969). However, since their technique used a narrower nozzle diameter, 10 μm *versus* 50 μm, the chance of nozzle clogging was greater (Heinzl & Hertz, 1985).

Instead of firing droplets in a continuous method, it is also possible to produce droplets when required, hence an impulse jet, or better known as drop-on-demand (DoD). In the late 1940s, Clarence Hansell invented the DoD device, at the Radio Corporation of America (Hansell, 1950). Figure 2 shows the schematics of his invention, which was never developed into a commercial product at that time. It took until 1971 when the Casio Company released the model *500 Typuter*, which was an electrostatic pull DoD device.
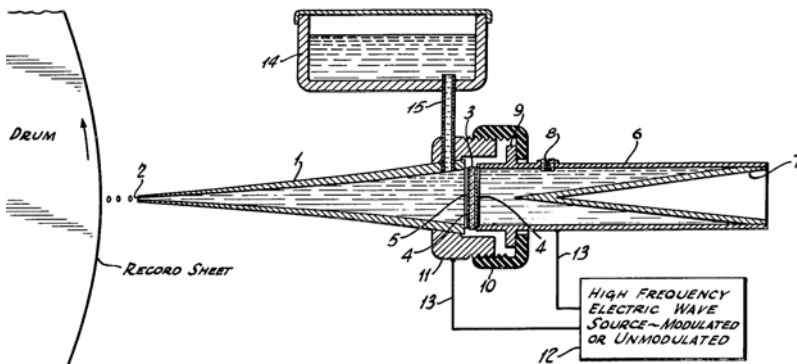

Fig. 2. Schematic drawing of the first drop-on-demand piezoelectric device. Reprinted from (Hansell, 1950).

Despite the fact that the basis of thermal inkjet (TIJ) DoD devices in the form of the sudden stream printer had already been developed in 1965 at the Sperry Rand Company (Naiman, 1965), this idea was picked up much later by the Canon company, when in 1979 they filed the patent for the first thermal inkjet printhead (Endo *et al.*, 1979). Simultaneously, Hewlett-Packard independently developed a similar technology that was first filed in 1981 (Vaught *et al.*, 1984). Thermal inkjet printers are actuated by a water vapour bubble, hence their name

bubble jet. The bubble is created by a thermal transducer that heats the ink above its boiling point and, thereby, causes a local expansion of the ink, resulting in droplet formation. The location of the thermal transducer can be either at the top of the reservoir – as used by HP – or at its side, which is the technique Canon uses.

At the beginning of the 1970s the piezoelectric inkjet (PIJ) DoD system was developed (Carnahan & Hou, 1970). At the Philips laboratories in Hamburg printers operating on the DoD principle were the subject of investigation for several years (Döring, 1982). In 1981 the *P2131* printhead was developed for the Philips *P2000T* microcomputer, which had a *Z80* microprocessor running at 2.5 MHz. Later the inkjet activities of Philips in Hamburg were continued under the spin-off company Microdrop (nowadays Microdrop Technologies, www.microdrop.com). The first piezoelectric DoD printer on the market was the serial character printer Siemens *PT80* in 1977.

Four different modes for droplet generation by means of a piezoelectric device were developed in the 1970s, which are summarised in Figure 3, and further explained below (Brünahl & Grishin, 2002).
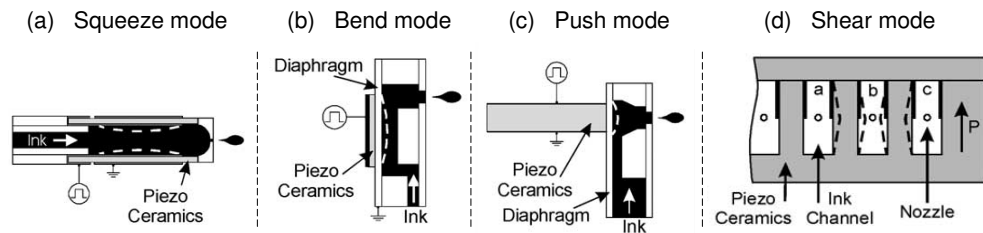

Fig. 3. Different piezoelectric drop-on-demand technologies. Reprinted from (Brünahl, 2002).

Firstly, the squeeze method, invented by Steven Zoltan (Zoltan, 1972), uses a hollow tube of piezoelectric material, that squeezes the ink chamber upon an applied voltage (Figure 3a). Secondly, the bend-mode (Figure 3b) uses the bending of a wall of the ink chamber as method for droplet ejection and was discovered simultaneously by Stemme of the Chalmers University in Sweden (Stemme, 1972) and Kyser of the Silonics company in the USA (Kyser & Sears, 1976). The third mode is the pushing method by Howkins (Figure 3c), where a piezoelectric element pushes against an ink chamber wall to expel droplets (Howkins, 1984). Finally, the shear-mode (Figure 3d) was found by Fishbeck, where the electric field is designed to be perpendicular to the polarization of the piezo-ceramics (Fishbeck & Wright, 1986).

Besides the continuous and drop-on-demand inkjet technique, a third type of inkjet printing is known, which is based on the electrostatic generation of ink droplets (Winston, 1962). The system is weakly pressurised, causing the formation of a convex meniscus of a conductive ink. An electrostatic force, which exceeds the meniscus' surface tension, is applied between the ink hemisphere and the flat electrode by setting a voltage. Depending on the nature of the electrical potential the system can either be a continuous or drop-on-demand inkjet: the pulse duration determines whether the ejected ink is a continuous stream or a stream of droplets. As a summary of the different inkjet printing technologies, Figure 4 schematically represents a classification thereof.

Inkjet Printing and Alternative Sintering of Narrow Conductive Tracks
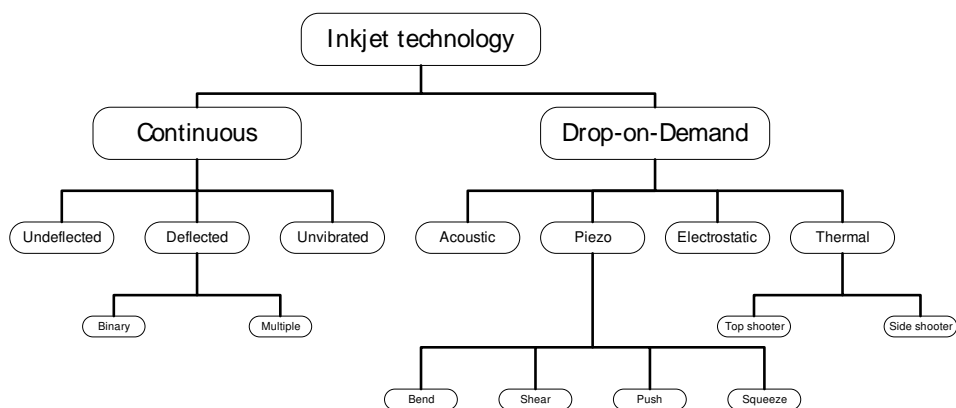on Flexible Substrates for Plastic Electronic Applications

269

Fig. 4. Classification of inkjet printing technologies, adapted from (Le, 1998).

Although inkjet printing offers a simple and direct method of electronic controlled writing with many advantages, including high speed production, silent, non-impact and fully electronic operation, inkjet printers failed to be commercially successful in their beginning: print quality as well as reliability and costs were hard to combine in a single printing technique. Whereas CIJ provides high throughput, it also requires high costs to gain good quality. Nowadays this technique is used in lower quality and high speed graphical applications such as textile printing and labelling. On the other hand, PIJ usually provides good quality but lacks high printing velocities: although this can be compensated for by using multi nozzle systems, but this increases the production costs as well. TIJ changed the image of inkjet printing dramatically. Not only could thermal transducers be manufactured in much smaller sizes, since they require a simple resistor instead of a piezoelectric element, but also at lower costs. Therefore, thermal inkjet printers dominate the colour printing market nowadays (Kipphan, 2004).

In scientific research piezoelectric DoD inkjet systems are mainly used because of their ability to dispense a wide variety of solvents, whereas thermal DoD printers are more compatible with aqueous solutions (Gans *et al.*, 2004). Furthermore, the rapid and localised heating of the ink within TIJ induces thermal stress on the ink. Nevertheless, research has been conducted using TIJ printers, for example to form conductive patterns, either by printing the water soluble conjugated polymer PEDOT:PSS (Yoshioka & Jabbour, 2006), or by printing aqueous solutions of conductive multi-walled carbon nanotubes (Kordás, 2006).

3. Methods for sintering nanoparticle inks

Conductive materials that are suitable for inkjet printing can be either solution-based or particle based. The former one is usually based on a metallo-organic decomposition (MOD) ink, in particular silver neodecanoate dissolved in an aromatic solvent (Dearden *et al.*, 2005; Smith *et al.*, 2006). These MOD inks have been used for inkjet printing since the late 1980s (Vest *et al.*, 1983). In order to obtain metal features, a conversion of organometallic silver inks is required, which usually takes place at relatively low temperatures below 200 °C (Wu *et al.*, 2007), although temperatures below 150 °C have been reported as well (Smith *et al.*, 2006, Perelaer *et al.*, 2009a). The typical metal loading of organometallic inks is 10 to 20 wt%.

In contrast to metal containing inks based on complexes, inks consisting of a dispersion of nanoparticles have been investigated as well, with the ability to have a silver loading >20 wt% being one of the reasons. Such a dispersion contains metallic nanoparticles with a diameter between 1 and 100 nm. It was found that gold nanoparticles with a diameter below 100 nm reveal a significant reduction in their melting temperature (Buffat & Borel, 1976), as depicted in Figure 5a from their bulk melting temperature of 1064 °C to well below 300 °C when the diameter is below 5 nm. Ten years later, Allen and co-workers showed that this reduction of the melting temperature is also valid for other metals, including tin, lead and bismuth (Allen *et al.*, 1986). In a graph of the melting temperature against the reciprocal of the particle radius the data exhibit near-linear relationships, as depicted in Figure 5b. It was also found that plates instead of spheres do not show a reduced melting temperature. This suggests that the size dependence of melting particles is related to the internal hydrostatic pressure caused by the surface stress and by the large surface curvature of the particles, but not by the planar surfaces of platelets.
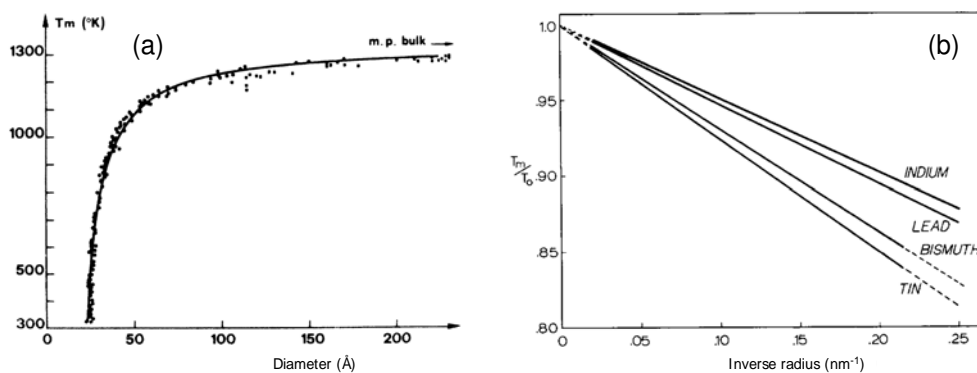

Fig. 5. Influence of the gold (a) and lead, bismuth, tin and indium (b) particle diameter on their melting temperature. Reprinted from (Buffat & Borel, 1976; Allen *et al.*, 1986), respectively.

Given the reduced melting temperature of nanoparticles, these particles represent ideal candidates for dispersion in a liquid medium and, subsequently, for inkjet printing. However, when two or more particles are in contact, merging of nanoparticles into larger clusters can take place due to the large surface curvature of the individual nanoparticles. This process is called sintering and takes place with small particles within the medium and at room temperature. Therefore, the nanoparticles have to be protected by a shell to prevent agglomeration in solution and to obtain a stable colloidal dispersion, as schematically depicted in Figure 6 (Lee *et al.*, 2006).

In non-polar solvents usually long alkyl chains with a polar head, like thiols, amines or carboxylic acids, are used to stabilise the nanoparticles (Perelaer *et al.*, 2008a). Steric stabilisation of these particles in non-polar solvents substantially screens van der Waals attractions and introduces steep steric repulsion between the particles at contact, which avoids agglomeration (Bönnemann & Richards, 2001). In addition, organic binders are often added to the ink to assure not only mechanical integrity and adhesion to the substrate, but also to promote the printability of the ink.

Inkjet Printing and Alternative Sintering of Narrow Conductive Tracks
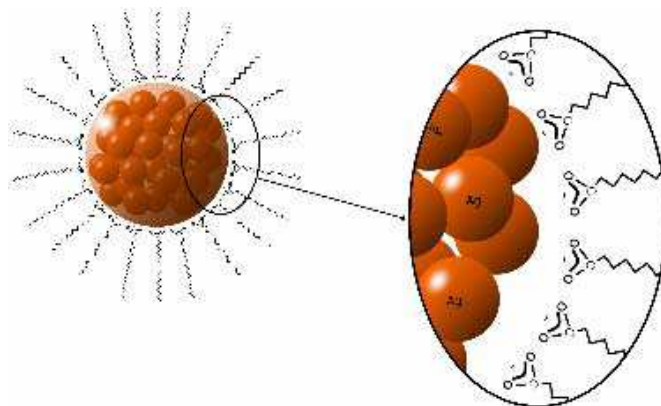on Flexible Substrates for Plastic Electronic Applications

271

Fig. 6. Schematic illustration of a silver nanoparticle with carboxylic acids as capping agent.

After silver containing inks have been inkjet printed, and solvent evaporation has occurred, another processing step is necessary to form conductive features since the organic shell inhibits close contact of the nanoparticles. Although evaporation of the solvent forces the particles close together, conductivity only arises when metallic contact between the particles is present and a continuous percolating network is formed throughout the printed feature. An organic layer between the silver particles as thin as a few nanometers is sufficient to prevent electrons moving from one particle to the other (Lovinger, 1979). The adsorbed dispersant stays on the surface of the particles and, typically, is removed by an increase in temperature.

Mostly, particulate features have been rendered conductive by applying heat. This thermal sintering method usually requires temperatures above 200 °C (Chou *et al.*, 2005). Other techniques that have been used to for conductive features include LASER sintering (Ko *et al.*, 2007), exposure to UV radiation (Radivojevic *et al.*, 2006), high temperature plasma sintering (Groza *et al.*, 1992) and pulse electric current sintering (Xie *et al.*, 2003). However, most of these techniques are not suitable for polymer substrate materials due to the large overall thermal energy impact. In particular, when using common polymer substrates, like polycarbonate (PC) and polyethylene terephthalate (PET), that have their glass transition temperature (Tg) well below the temperature required for sintering. In fact, only the expensive high-performance polymers, like polytetrafluoroethylene, polyetheretherketone and polyimide (PI) can be used at high temperatures, which represents a serious drawback for implementation in a large area production of plastic electronics and is not favourable in terms of costs.

In the field of sintering two properties are very important: firstly, the lowest temperature at which printed features become conductive, which is mainly determined by the organic additives in the ink (Liang *et al.*, 2004). Secondly, obtaining the lowest possible resistance of the printed features at the lowest possible temperature. To achieve a low resistance, sintering of the particles is required to transform the initially very small contact areas to thicker necks and, eventually, to a dense layer. High conductivities, hence low resistance, can then be obtained through the formation of large necks, which decrease constriction resistance and eventually form a metallic crystal structure with a low number of grain boundaries.

In the low temperature regime, the driving forces for sintering are mainly surface energy reduction due to the particles large surface-to-volume ratio, a process known as *Ostwald ripening* (Ostwald, 1896). This process triggers surface and grain boundary diffusion rather than bulk diffusion within the coalesced particles, as schematically depicted in Figure 7. Grain boundary diffusion allows for neck formation and neck radii increase, which is diminished by the energy required for grain boundary creation (Greer *et al.*, 2007). Therefore, the process will stall eventually, leaving a porous structure behind, which leads to lower conductivity values when compared to the bulk material.

1. Lattice diffusion (no densification)

2. Surface diffusion (no densification)

3. Through-lattice diffusion (densification)

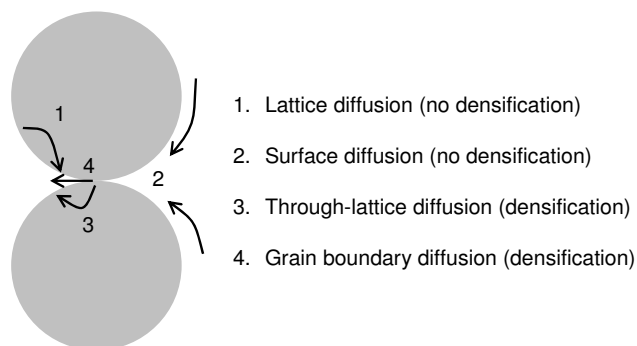4. Grain boundary diffusion (densification)

Fig. 7. A schematic representation of various atomic diffusion paths between two contacting particles. Paths 1 and 2 do not produce any shrinkage whilst paths 3 and 4 enable the sphere centres to approach one another, resulting in densification. Reprinted from (Greer *et al.*, 2007).

At high temperatures, however, lattice diffusion leads to closure of pores and densification. However, long sintering times are necessary for creating dense conductive features in a thermal process and obstruct the feasibility for an efficient industrial production processes.
In order to reduce production costs, alternative techniques that sinter silver nanoparticles in a selective manner without harming the underlying polymer substrate need to be found.
The properties of thermal sintering will be discussed in the next paragraphs, after which a technique that uses microwave radiation will be described as possible candidate for a selective sintering process.

3.1 Thermal sintering of inkjet printed silver lines

A major concern with printed electronics involves not only the control of the morphology of the tracks (Smith *et al.*, 2006; Berg *et al.*, 2007), but also the stability and adhesion of the obtained conductive tracks, although this has scarcely been investigated (Kim *et al.*, 2006). However, the main focus in plastic electronics lies in the low curing temperature of the conductive ink. For particle-based inks, the curing temperature is defined as the temperature where particles loose their organic shell and start showing conductance by direct physical contact. Whereas sintering (which is often mistakenly used instead of curing temperature) takes place at a higher temperature when all the organic material has been burnt off and necks begin to form between particles. The lowest temperature at which printed features become conductive is mainly determined by the organic additives in the ink (Liang *et al.*, 2004). Often high temperatures – typically up to 300 °C – are required to burn off the organic additives and to stimulate the sintering process to realise a more densely

Inkjet Printing and Alternative Sintering of Narrow Conductive Tracks
on Flexible Substrates for Plastic Electronic Applications

273

packed silver layer and a lower resistivity (Smith *et al.*, 2006; Yoshioka & Jabbour, 2006). It is therefore of utmost importance if further progress is to be made to identify an optimum between time, temperature and the obtained conductivity.

In order to reveal first structure-property relationships and to later develop the new ink, the sintering behaviour of inkjet printed silver tracks based on commercial inks was studied.

The critical curing temperature is defined in this case as the temperature at which the sample becomes conductive, *i.e.* having a resistance lower than 40 MΩ which is the upper measuring limit of the used multi-meter. Single lines with a length of 1 cm of the specific ink were inkjet printed onto boron-silicate glass and subsequently heated to 650 °C in an oven at a heating rate of 10 °C min^{-1}. During heating the resistance was measured online in a semi-continuous way, by measuring every 2 seconds. Using this dynamic scan approach, differences between the various inks can be determined.

Typical resistance results for the Cabot and Nippon inks are shown in Figure 8a and Figure 9a, respectively. The resistance of the lines for both inks decreases rapidly when heated above the critical curing temperature. The critical curing temperature for the Cabot silver ink is 194 °C, which is lower than the Nippon ink, 269 °C. According to the particle size measurements, 52.4 ± 11.0 nm for the Cabot ink and 10.8 ± 6.7 nm for the Nippon ink (see Figure 8b and Figure 9b), it was expected that the smaller particles would sinter at the lower temperature because of their higher sintering activity (Buffat & Borel, 1976; Allen *et al.*,
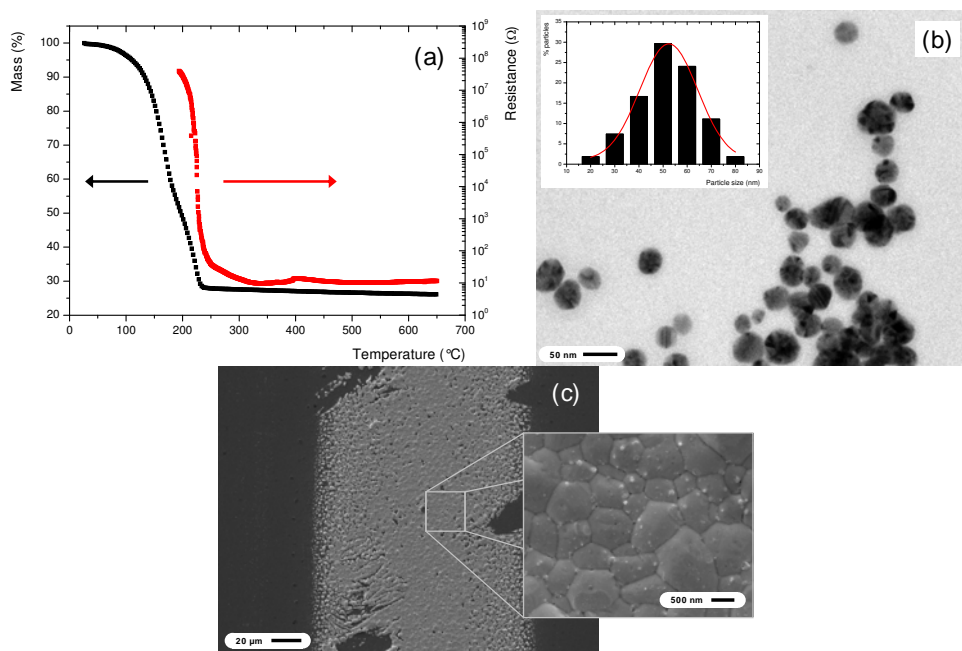

Fig. 8. Resistance over a single inkjet printed line with a length of 1 cm as function of temperature and thermogravimetric analysis (TGA) of Cabot silver ink (a). Transmission electron microscopy (TEM) image and particle size distribution of Cabot silver nanoparticles (b). Scanning electron microscopy (SEM) image of sintered Cabot silver nanoparticles at a temperature of 650 °C (c). Reprinted from (Perelaer et al., 2008a).

1986). This indicates that the organic additives in the ink strongly affect the critical curing temperature. Unfortunately, the nature of the organic additives in these commercially available inks is not disclosed.

To elaborate on this the mass decrease upon heating by means of thermogravimetric analysis (TGA) was also investigated. It should be mentioned that all inks have been dried prior to measuring by heating to 50 °C for 20 minutes, which removed volatile solvents. The TGA curve for Cabot silver ink shows a decrease of 72 wt%, which is not only the organic binder that is around each nanoparticle but also the non-volatile solvent ethylene glycol which is present in the ink (Figure 8a). The critical curing temperature corresponds to a temperature at which the initial sharp weight loss slows down. The first step in the removal of the organic materials has ended at this temperature. The steep decrease in resistance relates to the temperature range in which the last part of the organics is burnt off. Apparently, all organics have to be removed before the sintering of the Ag particles can proceed in a fast way. This is indicative of an additive that is strongly adsorbed on the surface of the silver particles.

The lines printed with the Nippon ink reveal a critical curing temperature and a fast decrease in resistance when only about 15% of the organic additives are removed (Figure 9a). Obviously, these particles can make metallic contact long before all the organics are gone. In addition, sintering proceeds very fast due to the small particle size. At the temperature where the organics have been completely burnt off, only a small additional decrease in resistance occurs. In this ink, only a minor part of the organic additives interferes with the sintering process but it does shift the critical curing temperature to a high value. For both inks, however, the resistance value levels off at a certain temperature. At this temperature all organics are burnt off and, apparently, the sintering process has ended and a silver layer with a final density and morphology has formed.

Figure 8c shows a scanning electron microscopy (SEM) image of a Cabot silver track that has been heated to 650 °C. As can be seen the particles have sintered to a dense continuous line.
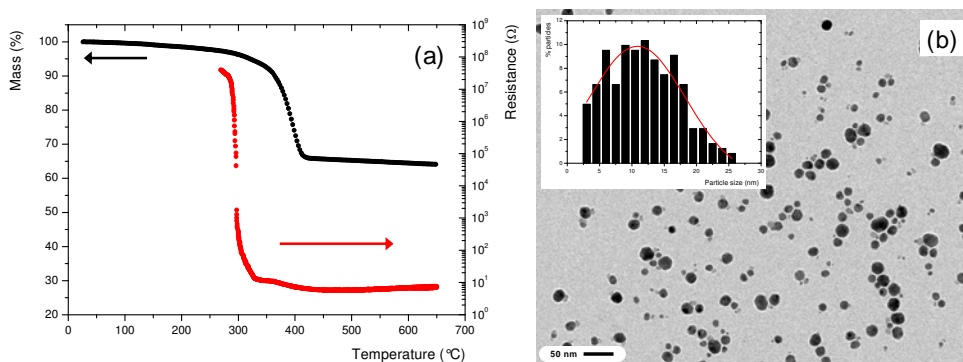

Fig. 9. Resistance over a single inkjet printed line with a length of 1 cm as function of temperature and thermogravimetric analysis (TGA) of Nippon silver ink (a). Transmission electron microscopy (TEM) image and particle size distribution of Nippon silver nanoparticles (b). Reprinted from (Perelaer et al., 2008a).

The electrical resistivity ρ of the inkjet printed lines was calculated after heating to 650 °C, using

Inkjet Printing and Alternative Sintering of Narrow Conductive Tracks
on Flexible Substrates for Plastic Electronic Applications

275

$$\rho = R \cdot A / \ell \tag{2}$$

with the lines resistance R, its length λ, and its cross sectional area A, and compared to the value of bulk silver (1.59×10^{-8} Ω m) (Fuller *et al.*, 2002). The resistivity was calculated to be 3.10×10^{-8} Ω m (51%) and 3.06×10^{-8} Ω m (52%) for Cabot and Nippon, respectively. The values in brackets indicate the percentage of conductivity ($1/\rho$) of bulk silver.

In summary, typical sintering temperatures of above 200 °C are required, which limits the usage of many potentially interesting substrate materials, such as common polymer foils or paper. Moreover, the long sintering time of 60 minutes or more that is generally required according to the ink supplier to create conductive features, also obstruct industrial implementation, e.g. roll-2-roll applications.

One selective technique for nanoparticle sintering that has been described in literature is based on an Argon ion LASER beam that follows the as-printed feature and selectively sinters the central region. Features with a line width smaller than 10 µm have been created with this technique (Ko *et al.*, 2007). However, the large overall thermal energy impact together with the low writing speed of 0.2 mm s^{-1} of the translational stage are limiting factors (Chung *et al.*, 2004). In fact, with this particularly technique low writing speeds are required for good electrical behaviour since the resistance increases for faster write speeds (Smith *et al.*, 2006). Thus, other techniques have to be used in order to facilitate fast and selective heating of the printed structures only. Microwave heating fulfils these requirements (Nüchter *et al.*, 2004).

3.2 Selective sintering of silver nanoparticle by using microwave radiation

Microwave heating is widely used for sintering of dielectric materials, conductive materials, and in synthetic chemistry (Wiesbrock *et al.*, 2004). It offers the advantage of uniform, fast and volumetric heating.

The dielectric response to a field is given by the complex permittivity

$$\varepsilon_r = \varepsilon' + i\varepsilon'' = \varepsilon' + i\frac{\sigma}{\omega \cdot \varepsilon_0} \tag{3}$$

where ε' accounts for energy storage, ε'' for energy loss of the incident electromagnetic wave or so-called dissipation, i the imaginary unit, σ the conductivity and ω the angular frequency. The ratio of the imaginary to the real part of the permittivity defines the capability of the material to dissipate power compared to energy storage and is generally know as the loss tangent:

$$\tan\delta = \frac{\varepsilon''}{\varepsilon'} \tag{4}$$

Depending on their loss characteristic, and thus their conductivity, materials can be opaque, transparent or an absorber. For bulk metals, being good electronic conductors, no internal electrical field is generated and the induced electrical charge remains at the surface of the sample (Agrawal, 2006). Consequently, metals reflect microwaves; while bulk metals do not absorb until they have been heated to about 500 °C, powders with particle sizes within the micrometer-region are rather good absorbers (Cheng, 1989). It is believed that the conductive particle interaction with microwave radiation, *i.e.* inductive coupling, is mainly based on Maxwell-Wagner polarisation, which results from the accumulation of charge at

the materials interfaces, electric conduction, and eddy currents. However, the main reasons for successful heating of metallic particles through microwave radiation are not yet fully understood.

The penetration depth d is defined as the distance into the material at which the incident power is reduced to $1/e$ (36.8%) of the surface value and is given by

$$d = \frac{c\varepsilon_0}{2\pi f \varepsilon''} = \frac{1}{\sqrt{\pi f \mu \sigma}} \qquad (5)$$

with c being the speed of light and f the frequency of the microwave radiation. Typically, highly conductive materials (*e.g.* metals) have a very small penetration depth. For example, the penetration depth of microwaves with a frequency of 2.45 GHz for metal powders of silver and copper is 1.3 and 1.6 μm, respectively. In contrast to the relatively strong microwave absorption by the conductive particles, the polarisation of dipoles in thermoplastic polymers below the Tg is limited, which makes the polymer foil's skin depth almost infinite, hence transparent, to microwave radiation.

Microwave sintering can only be successful if the dimension of the object perpendicular to the plane of incidence is of the order of the penetration depth. The average height of a single inkjet printed track of silver nanoparticles was measured to be 4.1 μm. The calculated penetration depth of the microwave irradiation into silver at a frequency of 2.45 GHz using equation (5) is only 1.3 μm. Therefore, it is to be expected that microwave heating will not be uniform throughout the complete line. However, since silver is a good thermal conductor in comparison to the polymer substrate, the silver tracks will be heated uniformly by thermal conductance.

Unsintered non-conductive silver lines were treated in a microwave reactor operating in constant power mode (300 W). The sintering times are significantly shortened in the microwave, from 60 minutes or more down to 240 seconds, as shown in Figure 10a. Within the reactor vessel the temperature reaches 200 °C, which is near the sintering temperature of 220 °C for conventional thermal sintering. Longer sintering times did not increase the conductivity, but sometimes resulted in deformation or decomposition of the substrate at the edges of the silver lines and the substrate.
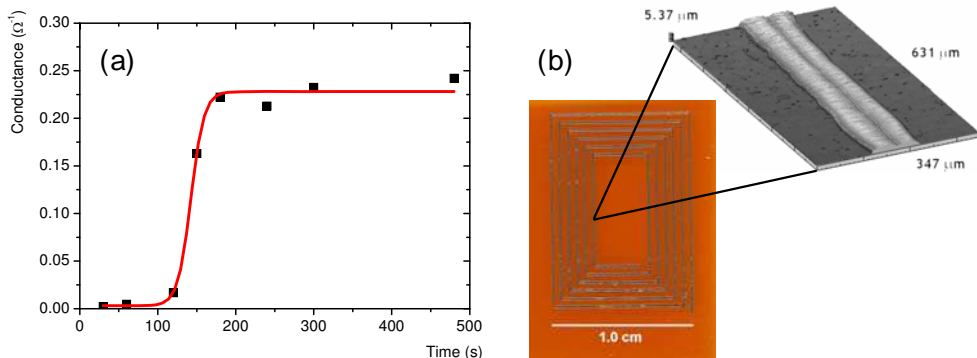

Fig. 10. Conductance as function of time for the microwave sintering of silver tracks (a) printed onto a polyimide substrate (b). Reprinted from (Perelaer et al., 2006).

Inkjet Printing and Alternative Sintering of Narrow Conductive Tracks
on Flexible Substrates for Plastic Electronic Applications

277

A typical resistivity value is 3.0×10^{-7} Ω m, which is approximately 20× the bulk silver value. With thermal sintering in an oven (220 °C, 60 minutes) similar values are obtained, which is in agreement to what is reported by other authors (Cheng *et al.*, 2005).

It was recently discovered that conductive antenna structures are more susceptible for absorption of microwaves than the printed feature by itself (Perelaer *et al.*, 2009b). Therefore, conductive antenna structures have been applied onto the polymer foil and were found to improve the sintering process, and thereby the obtained conductivity, significantly. These antennae were used both to measure the resistance of the single ink line and to capture the electromagnetic waves, which was possible since the electrodes were composed of particles that are able to absorb microwaves, as schematically depicted in Figure 11.

A single silver ink line was inkjet printed over the metallic probes and shortly cured in an oven for 1 to 5 minutes at a temperature of 110 °C. This relatively short time was chosen to stimulate solvent evaporation, but to minimize thermal curing. After this treatment, the single line had a relatively high resistance in the order of 10^2 to 10^4 Ω. The sample was subsequently exposed to microwave radiation for at least 1 second, while applying the lowest set-power of 1 W. This resulted in a pronounced decrease of the resistance of which the exact outcome depends on the initial resistance.
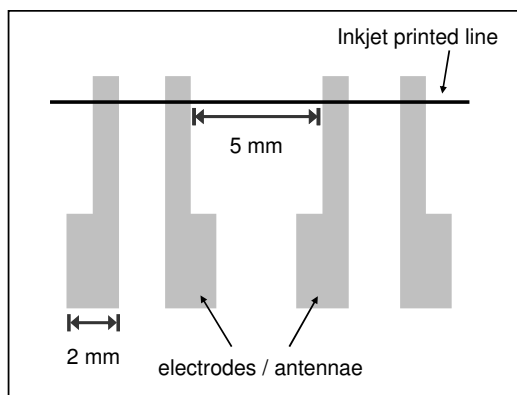
Fig. 11. Schematic representation of the printed template (a), with four silver electrodes/antennae in gray and a single silver line inkjet printed on top of the antennae in black. The total length of the line is 1.6 cm. Reprinted from (Perelaer et al., 2009b).

The *antenna effect*, which reflects the capability of absorbing microwaves into the material, was studied systematically by altering the surface area of the electrodes of the template. When increasing the size of the electrodes a rapid decrease of the resistance after microwave exposure was revealed, as is shown in Figure 12 for pre-dried samples. This may be explained by the improved absorption of the microwaves due to an increased surface area of the electrodes.

The antenna effect, however, is larger when the initial line resistance is small (Figure 12a), which is likely due to enhanced heat conduction from the electrodes to the ink line. For ink lines with an initially large resistance (Figure 12b), the energy transfer is still very effective, although the total antenna area has less impact on the final resistance. The data obtained in the absence of antennae ($A = 0$ mm²) clearly demonstrate that the energy absorption by the printed line is negligibly small at these short times.
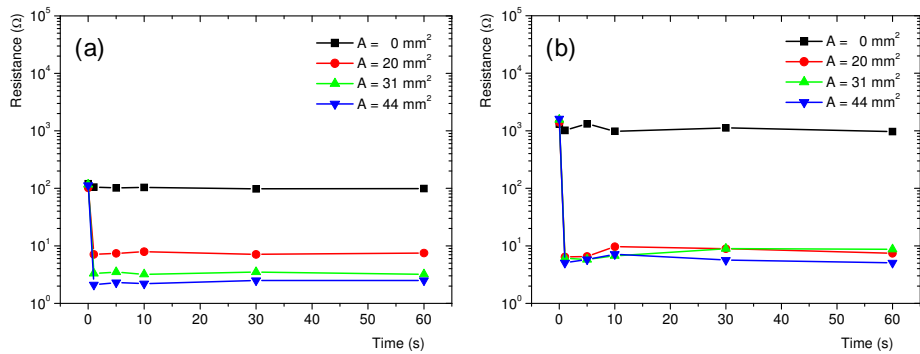
Fig. 12. Influence of the total surface of the four electrodes on the template for an initial line resistance of 100 Ω (b) and 1 kΩ (c) on microwave flash exposure for 1 to 60 seconds. Reprinted from (Perelaer et al., 2009b).

The absorption of microwave radiation may be improved by the presence of antennae due to a subsequently smaller impedance mismatch between air and sample. The intrinsic impedance Z of a circuit relative to free space is given by:

$$Z = Z_0 \sqrt{\varepsilon^*} \qquad (6)$$

where Z_0 is the impedance of free space (Z_0 = 377 Ω) and ε^* is the complex permittivity of the circuit relative to free space (Zuckermann & Miltz, 1994). The complex permittivity is related to the dielectric constant and the loss factor, according to equation (3), where the real part ε' is the ability of the material to store energy and where the imaginary part ε'' accounts for the losses via energy dissipation. The reflection, *i.e.* impedance mismatch Z/Z_0, scales with the square root of the complex permittivity ε^* and thus, in our experiments, with the resistance of the electrodes, which depends on their total surface area.

The electrical resistivity ρ of an inkjet printed line was subsequently calculated from equation 2. The conductivity ($1/\rho$) for the maximum surface area (44 mm²) of the antennae was found to be 34% when compared to the bulk silver value. A conductivity of 10% was revealed for the antennae with a surface area of 20 mm². This value, however, is significantly larger than the 5% that was reported in the previous section.

This process of flash sintering in the presence of conductive antenna structures may be implemented in a roll-to-roll production for sintering of inkjet printed silver tracks. The antennae do not need to make contact with the unsintered features, which makes recycling of the antennae possible; it was found that sintering took place even with a gap up to 0.5 cm between the antennae and the printed line. Increasing the distance reduces, however, the final conductivity. Thus, the antenna structures need to be close enough to the unsintered features, since the relay of electromagnetic waves is limited.

4. Improved resolution of direct inkjet printed conductive silver tracks on untreated polymer substrates

Another important aspect of conductive tracks, besides their conductivity properties, is the tracks dimensions, in particular the width of the track, hence the resolution of the printed feature. Typical dimensions of inkjet printed features depend on the nozzle diameter and

Inkjet Printing and Alternative Sintering of Narrow Conductive Tracks
on Flexible Substrates for Plastic Electronic Applications

279

are usually not below 100 µm. The most obvious way to minimise the feature size, *i.e.* line width, is by reducing the nozzle diameter (Le, 1998). However, this introduces a narrow window with respect to the applicable surface tension and viscosity of the inks, and thereby, the range of inks that can be printed. Furthermore, when printing dispersions the particles should be sufficiently smaller than the nozzle diameter; otherwise nozzle clogging occurs. When using piezo-electric based DoD inkjet printers, smaller droplets can also be produced by modifying the waveform (Chen & Basarana, 2002).

Other techniques to minimise feature sizes include an increased substrate's temperature, which will stimulate solvent evaporation and leave smaller droplets on the substrate due to a limited spreading (Perelaer *et al.*, 2006), and fluid-assisted dewetting effects (Dockendorf *et al.*, 2006). The latter and relatively new method was described as follows: a line of gold nanoparticle dispersion in toluene was deposited on a glass substrate, after which a water droplet was dispensed over the line. Subsequently, the pattern shrank due to a transport of the toluene from the gold dispersion into the water region, triggered by controlled heat addition from the substrate, whose temperature was set to 95 °C. Toluene and water are practically immiscible at room temperature, but at this temperature toluene mixes very well with water. During the dewetting phase, the three-phase-contact line is pulled by the uncompensated Young's force. Furthermore, the authors explain the dewetting dynamics by the action of thermocapillarity enhanced by the convection microflow generated in the water layer.

Much research has been done on predefined (surface energy) patterns on a substrate that forces material to remain in a preferred area on the surface (Menard *et al.*, 2007; Hendriks *et al.*, 2008; Sirringhaus *et al.*, 2000). These techniques rely on the use of expensive masks and conventional photolithography, which subsequently increases production costs. To reduce these costs a method to produce narrow conductive silver tracks without pre-patterning or modifying the surface energy of the substrate is required. Preferably, the substrate's surface energy should not be too low, because printing then introduces bulges into the printed features (Duineveld, 2003), for example with polytetrafluoroethylene (PTFE) foils, as can be seen on the left-hand side in Figure 13. Commonly used polymer substrates, like polyethylene terephthalate (PET) or polyimide (PI), have a relatively high surface energy, shown on the right-hand side in Figure 13. Although printing on these substrates leads to continuous and straight lines, broad lines are obtained over the whole printed feature, due to the relatively good wetting of the solvent with the substrate. Moreover, unwanted drying effects, such as the coffee ring effect may appear (Deegan *et al.*, 2000; Soltman & Subramanian, 2008). Clearly, an optimum between surface energy and solvent is necessary. Polyarylate polymer foils fulfil this need, since they have a surface energy between the value of PTFE and PI.

The silver ink from Cabot (Cabot Printing Electronics and Displays, Albuquerque, USA) has been inkjet printed using a cartridge able to dispense droplets with a volume as small as 1 pL. Besides a decrease in nozzle size, and thus a higher print resolution, further decrease in line diameter was realised by heating the sample holder of the printer to its maximum temperature (60 °C), which stimulates the evaporation of the solvent and prevents broadening of the lines (Perelaer *et al.*, 2006).

Figure 14a shows the dependency of line width on dot spacing; a decrease in line width is observed when the dot spacing is increased. Obviously, with increased dot spacing less material is deposited per unit length, resulting in smaller structures. Partially continuous lines were formed, when a dot spacing larger than 25 µm was used and further increase led
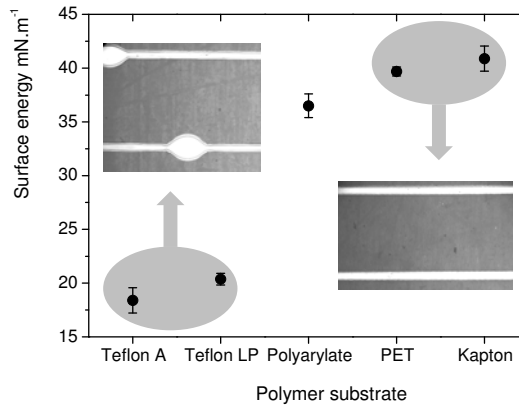
Fig. 13. Surface energy of five commercially available polymer substrates and an impression of the printed lines on these surfaces. Reprinted from (Osch et al., 2008).
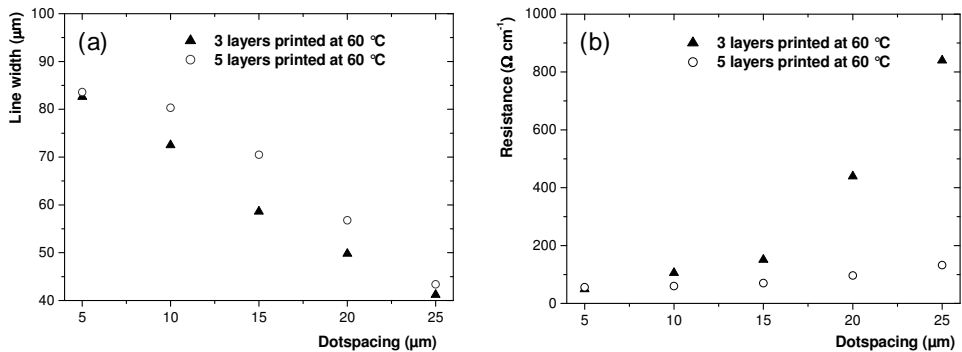

Fig. 14. Line width (a) and resistance (b) as function of dot spacing for three and five layers subsequently printed on top of each other. Reprinted from (Osch et al., 2008).

to individual droplets. Therefore, using a dot spacing of 25 μm resulted in the smallest line width of 40 μm, which corresponds to a resolution of approximately 600 dots per inch.[1]

In the same way, the resistance will increase when the dot spacing is increased, as depicted in Figure 14b. However, the number of layers printed on top of each other strongly influences the dependency. The resistance of lines consisting of 3 layers strongly increases with dot spacing, whereas the resistance shows a much more gradual increase with dot spacing when 5 layers are printed on top. This can be explained by the formation of more parallel percolating pathways when more material is deposited per unit length.

Typical dimensions of printed silver tracks onto polyarylate films are shown in Figure 15. Inkjet printed features on polyarylate foil with a line width of 85 μm and 40 μm without any defects such as bulges or coffee drop effects were obtained using a dot spacing of 5 μm (a) and 25 μm (b), respectively. The silver lines were sintered after drying in an oven at 200 °C for 1 hour. Subsequently, the resistance was measured by using the 4-point method. The

---

[1] 600 dots per inch (DPI) correspond to a single dot diameter of 2.54/600 cm = 42.3 μm.

Inkjet Printing and Alternative Sintering of Narrow Conductive Tracks
on Flexible Substrates for Plastic Electronic Applications

281

conductivity ($1/\rho$) was 23% of the bulk silver value for tracks printed with a dot spacing of 5 µm and 13% when using a dot spacing of 25 µm.
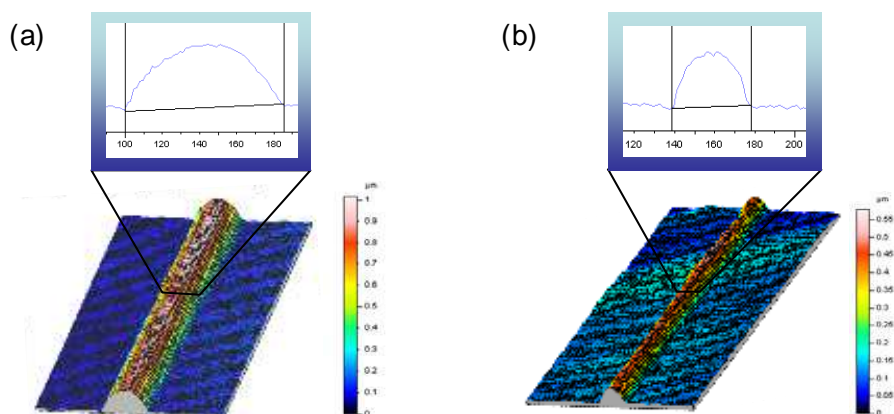

Fig. 15. Cross-sectional image and 3D image of inkjet printed silver tracks on polyarylate films using a dot spacing of 5 µm (a) and 25 µm (b). The substrate was heated to 60 °C and five layers were printed on top of each other. Reprinted from (Osch et al., 2008).

5. Conclusions and outlook

In order to develop better and alternative sintering methods, a basic understanding of thermal sintering and how particles sinter has been described. The conductivity development of commercially available silver inks has been discussed. Hereto, the resistance was measured on-line during the heating of the silver tracks from room temperature to 650 °C. The standard method, however, for sintering is by applying heat, typically above 200 °C, which is not compatible with the common polymer foils that are being considered as substrates for plastic electronics applications.

By using microwave radiation instead of conventional radiation-conduction-convection heating, the sintering time of silver nanoparticles was shortened by a factor of 20, *i.e.* instead of 60 minutes three minutes were sufficient for sintering. The polymer substrate is virtually transparent to microwave radiation, whereas the conductive silver nanoparticles absorb the microwaves strongly and sinter.

Furthermore, the presence of conductive antennae promotes nanoparticle sintering in pre-cured ink lines to an extent that depends on the total area of the antennae. For cured nanoparticle inks that are connected to antennae, sintering times of 1 second are sufficient to obtain pronounced nanoparticle sintering. The antenna effect is greater if the ink line already exhibits conductivity. It is believed that this is due to the decreased mismatch between the impedance of air and sample. Using metal antennae, it was revealed that 1 second is sufficient to obtain pronounced sintering by microwave heating. The degree of sintering for these short exposure periods, however, strongly depends on the initial resistance of the pre-cured ink lines. After microwave flash sintering, the tracks revealed conductivity values of 10 to 34% compared to the bulk silver value, which is significantly higher compared to conventional heating methods.

The procedure of printing and subsequently microwave flash sintering can be used, for example, in roll-to-roll (R2R) production applications, such as large area fabrication of RFID tags or solar cells. Its major advantage pertains to both the high process speed and the low processing temperature, which reduce processing costs, as common polymer foils like polyethylene naphthalate (PEN) can be used.

Very recently, another alternative sintering technique has been reported that uses a low pressure argon plasma exposure (Reinhold *et al.*, 2009). Typical resistivity values of 2.5 to 3× the bulk silver value were achieved. The process shows an evolution starting from a sintered top layer into bulk material, which determines the resistivity of the sintered material. Through-sintering does not occur with greater thicknesses than the penetration depth of the plasma species.

Several techniques have been discussed to improve the resolution of inkjet printed features. In order to reach the smallest line width for printed silver tracks, it is necessary to tune the ink surface tension to the substrates energy, hence its wettability. Furthermore, dot spacing, surface temperature and in-flight droplet diameter strongly affect the resolution as well and need to be optimised.

In general, it can be concluded that inkjet printing is capable of preparing high-resolution conductive features on polymer substrates. Together with inkjet printing, (ink) materials can be saved, since the ink is only dispensed on demand. It is, however, necessary to tune the polymer substrate as well the conductive inks properties. Alternative and selective sintering methods open new routes to produce conductive features on common polymer foils that have a relatively low glass transition temperature. This combination may be then employed in roll-to-roll printed plastic microelectronic devices.

6. References

Agrawal, D. (2006). Microwave sintering of ceramics, composites and metallic materials, and melting of glasses. *Trans. Ind. Ceram. Soc.*, 65, 129-144.

Allen, G. L.; Bayles, R. A.; Gile, W. W. & Jesser, W. A. (1986). Small particle melting of pure metals. *Thin Solid Films*, 144, 297-308.

Attinger, D.; Zhao, Z. & Poulikakos, D. (2000). An experimental study of molten microdroplet surface deposition and solidification: transient behavior and wetting angle dynamics. *J. Heat Transfer*, 122, 544-556.

Berg, van den, A. M. J.; Laat, de, A. W. M.; Smith, P. J.; Perelaer, J. & Schubert, U. S. (2007a). Geometric control of inkjet printed features using a gelating polymer. *J. Mater. Chem.*, 17, 677-683.

Bogy, D. B. (1979). Drop formation in a circular liquid jet. *Ann. Rev. Fluid. Mech.*, 11, 207-228.

Bönnemann, H. & Richards, R. M. (2001). Nanoscopic metal particles – synthetic methods and potential applications. *Eur. J. Inorg. Chem.*, 2455-2480.

Brünahl, J. & Grishin, A. M. (2002). Piezoelectric shear mode drop-on demand inkjet actuator. *Sens. Actuators A*, 101, 371-382.

Buffat, P. & Borel, J.-P. (1976). Size effect on the melting temperature of gold particle. *Phys. Rev. A*, 13, 2287-2298.

Carnahan, R. D. & Hou, S. L. (1977). Inkjet technology. *IEEE Trans. Ind. Appl.*, IA-13, 95-105.

Chen, A. U. & Basaran, O. A. (2002). A new method for significantly reducing drop radius without reducing nozzle radius in drop-on-demand drop production. *Phys. Fluids*, 14, L1-L4.

Inkjet Printing and Alternative Sintering of Narrow Conductive Tracks
on Flexible Substrates for Plastic Electronic Applications

283

Cheng, D. K. (1989). *Field and Wave Electromagnetics*, Addison-Wesley Co. Inc., ISBN 0-201-12819-5, Reading.

Cheng, K.; Yang, M.-H.; Chiu, W. W. W.; Huang, C.-Y.; Chang, J.; Ying, T.-F. & Yang, Y. (2005). Ink-jet printing, self-assembled polyelectrolytes, and electroless plating: low cost fabrication of circuits on a flexible substrate at room temperature. *Macromol. Rapid Commun.*, 26, 247-264.

Chou, K.-S.; Huang, K.-C. & Lee, H.-H. (2005). Fabrication and sintering effect on the morphologies and conductivity of nano-Ag particle films by the spin coating method. *Nanotechnology*, 16, 779-784.

Chung, J.; Bieri, N. R.; Ko, S.; Grigoropoulos, C. P. & Poulikakos, D. (2004). In-tandem deposition and sintering of printed gold nanoparticle inks induced by continuous gaussian laser irradiation. *Appl. Phys. A*, 79, 1259-1261.

Cuk, T.; Troian, S. M.; Hong C. M. & Wagner, S. (2000). Using convective flow splitting for the direct printing of fine copper lines. *Appl. Phys. Lett.*, 77, 2063-2065.

Dearden, A. L.; Smith, P. J.; Shin, D.-Y.; Reis, N.; Derby, B. & O'Brien, P. (2005). A low curing temperature silver ink for use in ink-jet printing and subsequent production of conductive tracks. *Macromol. Rapid Commun.*, 26, 315-318.

Deegan, R. D.; Bakajin, O.; Dupont, T. F.; Huber, G.; Nagel, S. R. & Witten, T. A. (2000). Contact line deposits in an evaporating drop. *Phys. Rev. E*, 62, 756-765.

Derby, B. (2008). Bio printing: inkjet printing proteins and hybrid cell-containing materials and structures. *J. Mater. Chem.*, 18, 5717-1521.

Dockendorf, C. P. R.; Choi, T.-Y.; Poulikakos, D. & Stemmer, A. (2006). Size reduction of nanoparticle ink patterns by fluid-assisted dewetting. *Appl. Phys. Lett.*, 88, 131903 (3 pp).

Döring, M. (1982). Inkjet printing. *Philips Tech. Rev.*, 40, 192-198.

Duineveld, P. C. (2003). The stability of ink-jet printed lines of liquid with zero receding contact angle on a homogeneous substrate. *J. Fluid Mech.*, 477, 175-200.

Elmqvist, R. (1951). Measuring instrument of the recording type. US Patent 2,566,443.

Endo, I.; Sato, Y.; Saito, S.; Nakagiri, T. & Ohno, S. (1979). Liquid jet recording process and apparatus therefor. GB Patent 2,007,162.

Fishbeck, K. H. & Wright, A. T. (1986). Shear mode transducer for drop-on-demand liquid ejector. US Patent 4,584,590.

Forrest, S. R. (2004). The path to ubiquitous and low-cost organic electronic appliances on plastic. *Nature*, 428, 911-918.

Fuller, S. B.; Wilhelm E. J. & Jacobson, J. M. (2002). Inkjet printed nanoparticle microelectromechanical systems. *J. Microelectromech. Syst.*, 11, 54-60.

Gamerith, S.; Klug, A.; Schreiber, H.; Scherf, U.; Moderegger E. & List, E. J. W (2007). Direct ink-jet printing of Ag-Cu nanoparticle and Ag-precursor based electrodes for OFET applications. *Adv. Funct. Mater.*, 17, 3111-3118.

Gans, de, B.-J; Duineveld, P. C. & Schubert, U. S. (2004). Inkjet printing of polymers: state of the art and future developments. *Adv. Mater.*, 16, 203-213.

Gans, de, B.-J. &. S. Schubert, U. S. (2004). Inkjet printing of well-defined polymer dots and arrays. *Langmuir*, 20, 7789-7793.

Goedde, E. F. & Yuen, M. C. (1970). Experiments on liquid jet instability. *J. Fluid Mech.*, 40, 495-511.

Greer, J. R. & Street, R. A. (2007). Thermal cure effects on electrical performance of nanoparticle silver inks. *Acta Mater.*, 55, 6345–6349.

Groza, J. R.; Risbud, S. H. & Yamazaki, K. (1992). Plasma activated sintering of additive-free AlN powders to near-theoretical density in 5 minutes. *J. Mater. Res.*, 7, 2643-2645.

Hansell, C. W. (1950). Jet sprayer actuated by supersonic waves. US Patent 2,512,743.

Heinzl, J. & Hertz, C. H. (1985). Ink-jet printing. *Adv. Electron. Electron Phys.*, 65, 91-171.

Hendriks, C. E.; Smith, P. J.; Perelaer, J.; Berg, van den, A. M. J. & Schubert, U. S. (2008). "Invisible" silver tracks produced by combining hot-embossing and inkjet printing. *Adv. Funct. Mater.*, 18, 1031-1038.

Hertz, C. H. & Simonsson, S.-I. (1969). Intensity modulation of ink-jet oscillographs. *Med. & Biol. Eng.*, 7, 337-340.

Hong, C. M. & Wagner, S. (2000). Inkjet printed copper source/drain metallization for amorphous silicon thin-film transistors. *IEEE Electron Device Letters*, 21, 384-386.

Howkins, S. D. (1984). Inkjet method and apparatus. US Patent 4,459,601.

Huang, D.; Liao, F.; Molesa, S.; Redinger, D. & Subramanian, V. (2004). An ink-jet-deposited passive component process for RFID. *IEEE Trans. Electron Devices*, 51, 1978-1983.

Kamphoefner, F. J. (1972). Inkjet printing. *IEEE Trans. Electron Devices*, 19, 584-593.

Keeling, M. R. (1981). Inkjet printing. *Phys. Technol.*, 12, 196-203.

Kim, D.; Jeong, S.; Park, B. K. & Moon, J. (2006). Direct writing of silver conductive patterns: imporvement of film morphology and conductance by controlling solvent compositions. *Appl. Phys. Lett.*, 89, 264101 (3 pp).

Kim, D.; Jeong, S.; Lee, S.; Kyun Park, B. & Moon, J. (2007). Organic thin film transistor using silver electrodes by the inkjet printing technology. *Thin Solid Films*, 515, 7692-7696.

Kipphan, H. (2004). *Handbook of print media: Technologies and manufacturing processes*, Springer, ISBN 3-540-67326-1, Berlin.

Ko, S. H.; Pan, H.; Grigoropoulos, C. P.; Luscombe, C. K.; Fréchet, J. M. J. & Poulikakos, D. (2007). All-inkjet-printed flexible electronics fabrication on a polymer substrate by low-temperature high-resolution selective laser sintering of metal nanoparticles. *Nanotechnology*, 18, 345202 (8 pp).

Kordás, K.; Mustonen, T.; Tóth, G.; Jantunen, H.; Lajunen, M.; Soldano, C.; Talapatra, S.; Kar, S.; Vajtai, R. & Ajayan, P. M. (2006). Inkjet printing of electrically conductive patterns of carbon nanotubes. *Small*, 2, 1021-1025.

Kyser, E. L. & Sears, S. B. (1976). Method and apparatus for recording with writing fluids and drop projection means therefore. US Patent 3,946,398.

Lee, K. J.; Jun, B. H.; Kim, T. H. & Joung, J. (2006). Direct synthesis and inkjetting of silver nanocrystals toward printed electronics. *Nanotechnology*, 17, 2424-2428.

Le, H. P. (1998). Progress and trends in ink-jet printing technology. *J. Imaging Sci. Technol.*, 42, 49-62.

Liang, L. H.; Shen, C. M.; Du, S. X.; Liu, W. M.; Xie, X. C. & Gao, H. J. (2004). Increase in thermal stability induced by organic coatings on nanoparticles. *Phys. Rev B.*, 70, 205419 (5 pp).

Liu, J. G.; Chen, C. H.; Zheng, J. S. & Huang, J. Y. (2005). CO_2 laser direct writing of silver lines on epoxy resin from solid film. *Appl. Surf. Sci.*, 245, 155-161.

Lovinger, A. J. (1979). Development of electrical conduction in silver-filled epoxy adhesives. *J. Adhesion*, 10, 1-15.

Menard, E.; Meit, M. A.; Sun, Y.; Park, J.-U.; Jay-Lee Shir, D.; Nam, Y.-S.; Jeon, S. & Rogers, J. A. (2007). Micro- and nanopatterning techniques for organic electronic and optoelectronic systems. *Chem. Rev.*, 107, 1117-1160.

Molesa, S.; Redinger, D. R.; Huang, D. C. & Subramanian, V. (2003). High-quality inkjet-printed multilevel interconnects and inductive components on plastic for ultra-low-cost RFID applications. *Mat. Res. Soc. Symp. Proc.*, 769, H8.3.1-H8.3.6.

Naiman, M. (1965). Sudden stream printer. US Patent 3,179,042.

Nollet, J.-A. & Watson, W. (1749). Recherches sur les causes particulieres des phénoménes électriques, et sur les effects nuisibles ou avantageux qu'on peut en attendre. *Philos. Trans.*, 46, 368-397.

Nüchter, M.; Ondruschka, B.; Bonrath, W. & Gum, A. (2004). Microwave assisted synthesis - a critical technology overview. *Green Chem.*, 6, 128-141.

Osch, van, T. H. J.; Perelaer, J.; Laat, de, A. W. M. & Schubert, U. S. (2008). Inkjet printing of narrow conductive tracks on untreated polymeric substrates. *Adv. Mater.*, 20, 343-345.

Ostwald, W. (1896). *Lehrbruck der Allgemeinen Chemie*, Vol. 2, Part 1, Leipzig.

Perelaer, J.; Gans, de, B.-J. & Schubert, U. S. (2006). Ink-jet printing and microwave sintering of conductive silver tracks. *Adv. Mater.*, 18, 2101-2104.

Perelaer, J.; Laat, de, A. W. M.; Hendriks, C. E. & Schubert, U. S. (2008a). Inkjet-printed silver tracks: low temperature curing and thermal stability investigation. *J. Mater. Chem.*, 18, 3209-3215.

Perelaer, J.; Smith, P. J.; Hendriks, C. E.; Berg, van den, A. M. J. & Schubert, U. S. (2008b). The preferential deposition of silica micro-particles at the boundary of inkjet printed droplets. *Soft Matter*, 4, 1072-1078.

Perelaer, J.; Hendriks, C. E.; Laat, de, A. W. M. & Schubert, U. S. (2009a). One-step inkjet printing of conductive silver tracks on polymer substrates. *Nanotechnology*, 20, 165303 (5 pp).

Perelaer, J.; Klokkenburg, M.; Hendriks, C. E. & Schubert, U. S. (2009b). Microwave flash sintering of inkjet printed silver tracks on polymer substrates. *Adv. Mater.*, 21, 4830-4834.

Potyrailo, R. A.; Surman, C. & Morris, W. G. (2009). Combinatorial screening of polymeric sensing materials using RFID sensors: combined effects of plasticizers and temperature. *J. Comb. Chem.*, 11, 598-603.

Reinhold, I.; Hendriks, C. E.; Eckardt, R.; Kranenburg, J. M.; Perelaer, J.; Baumann, R. R. & Schubert, U. S. (2009). Argon plasma sintering of inkjet printed silver tracks on polymer substrates. *J. Mater. Chem.*, 19, 3384-3388.

Reis, N.; Ainsley, C. & Derby, B. (2005). Ink-jet delivery of particle suspensions by piezoelectric droplet ejectors. *J. Appl. Phys.*, 97, 094903 (6 pp).

Radivojevic, Z.; Andersson, K.; Hashizume, K.; Heino, M.; Mantysalo, M.; Mansikkamaki, P.; Matsuba, Y. & Terada, N. (2006). Optimised curing of silver ink jet based printed traces. *Proceedings of 12th Intl. Workshop on Thermal investigations of ICs*, pp. 133-138, ISBN 2-916187-04-9, Nice, September 2006, TIMA Editions, Nice.

Rayleigh, L. (1878). On the instability of jets. *Proc. London Math. Soc.*, 10, 4-13.

Savart, F. (1833). Mémoires sur la constitution des veines liquides lancées par des orifices circulaires en mince paroi. *Ann. Chim. Phys.*, 53, 337-386.

Schmid, G. (2004). *Nanoparticles: from theory to applications*, Wiley, ISBN 3-527-30507-6, Weinheim.

Szczech, J. B. Megaridis, C. M. Gamota D. R. & Zhang, J. (2002). Fine-line conductor manufacturing using drop-on-demand PZT printing technology. *IEEE Trans. Electron. Pack.*, 25, 26-33.

Shim, G. H.; Han, M. G.; Sharp-Norton, J. C.; Creager, S. E. & Foulger, S. H. (2008). *J. Mater. Chem.*, 18, 594-601.

Sirringhaus, H.; Kawase, T.; Friend, R. H.; Shimoda, T.; Inbasekaran, M.; Wu, W. & Woo, E. P. (2000). High-resolution inkjet printing of all-polymer transistor circuits. *Science*, 290, 2123-2126.

Smith, P. J.; Shin, D.-Y.; Stringer, J. E.; Reis, N. & Derby, B. (2006). Direct inkjet printing and low temperature conversion of conductive silver patterns. *J. Mater. Sci.*, 41, 4153-4158.

Soltman, D. & Subramanian, V. (2008). Inkjet-printed line morphologies and temperature control of the coffee ring effect. *Langmuir*, 24, 2224-2231.

Stemme, N. G. E. (1972). Arrangement of writing mechanics for writing on paper with a colored liquid. US Patent 3,747,120.

Sweet, R. G. (1965). High frequency recording with electrostatically deflected ink jets. *Rev. Sci. Instr.*, 36, 131-136.

Tekin, E.; Smith, P. J. & Schubert, U. S. (2008). Inkjet printing as a deposition and patterning tool for polymers and inorganic particles. *Soft Matter*, 4, 703-713.

Thomson, W. (1867). Improvements in telegraphic receiving and recording instruments. UK Patent 2,147.

Vaught, J. L.; Cloutier, F. L.; Donald, D. K.; Meyer, J. D.; Tacklind, C. A. & Taub, H. H. (1984). Thermal ink-jet printer. US Patent 4,490,728.

Vest, R. W.; Tweedell, E. P. & Buchanan, R. C. (1983). Inkjet printing of hybrid circuits. *Intl. J. Hybrid Microelectron.*, 6, 261-267.

Wiesbrock, F.; Hoogenboom, R. & Schubert, U. S. (2004). Microwave-assisted polymer synthesis: state-of-the-art and future prospectives. *Macromol. Rapid Commun.*, 25, 1739-1764.

Winston, C. R. (1962). Method and aparatus for transfering ink. US Patent 3,060,429.

Wu, Y.; Li, Y. & Ong, B. S (2007). A simple and effective approach to a printable silver conductor for printed electronics. *J. Am. Chem. Soc.*, 129, 1862-1863.

Xie, G.; Ohashi, O.; Yamaguchi, N. & Wang, A. (2003). Effect of surface oxide films on the properties of pulse electric-current sintered metal powders. *Metall. Mater. Trans. A*, 34A, 2655-2661.

Yoshioka, Y. & Jabbour, G. E. (2006). Desktop inkjet printer as a tool to print conducting polymers. *Synth. Met.*, 156, 779-783.

Zoltan, S. I. (1972). Pulsed droplet ejecting system. US Patent 3,683,212.

Zuckerman, H. & Miltz, J. (1994). Changes in thin-layer susceptors during microwave. *Packag. Technol. Sci.*, 7, 21-26.
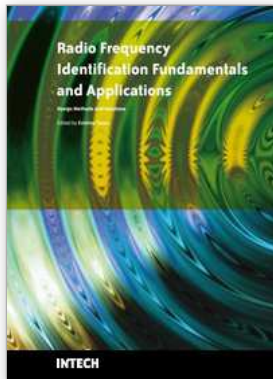
Radio Frequency Identification Fundamentals and Applications
Design Methods and Solutions
Edited by Cristina Turcu

This book, entitled Radio Frequency Identification Fundamentals and Applications, Bringing Research to Practice, bridges the gap between theory and practice and brings together a variety of research results and practical solutions in the field of RFID. The book is a rich collection of articles written by people from all over the world: teachers, researchers, engineers, and technical people with strong background in the RFID area. Developed as a source of information on RFID technology, the book addresses a wide audience including designers for RFID systems, researchers, students and anyone who would like to learn about this field. At this point I would like to express my thanks to all scientists who were kind enough to contribute to the success of this project by presenting numerous technical studies and research results. However, we couldn't have published this book without the effort of InTech team. I wish to extend my most sincere gratitude to InTech publishing house for continuing to publish new, interesting and valuable books for all of us.

How to reference
In order to correctly reference this scholarly work, feel free to copy and paste the following:

Jolke Perelaer and Ulrich S. Schubert (2010). Inkjet Printing and Alternative Sintering of Narrow Conductive Tracks on Flexible Substrates for Plastic Electronic Applications, Radio Frequency Identification Fundamentals and Applications Design Methods and Solutions, Cristina Turcu (Ed.), ISBN: 978-953-7619-72-5, InTech, Available from: http://www.intechopen.com/books/radio-frequency-identification-fundamentals-and-applications-design-methods-and-solutions/inkjet-printing-and-alternative-sintering-of-narrow-conductive-tracks-on-flexible-substrates-for-pla

INTECH
open science | open minds